J|A|C|S
ARTICLES
Published on Web 12/28/2007

The Chemical Bond between Au(I) and the Noble Gases. Comparative Study of NgAuF and $NgAu^+$ (Ng = Ar, Kr, Xe) by Density Functional and Coupled Cluster Methods

Leonardo Belpassi,*,§ Ivan Infante,‡ Francesco Tarantelli,§ and Lucas Visscher||

Dipartimento di Chimica e I.S.T.M.-C.N.R., Universita' di Perugia, 06123, Perugia, Italy, Department of Physical Chemistry, University of Geneva, 30 Quai Ernest Ansermet, CH-1211 Geneva, Switzerland, and Section Theoretical Chemistry, Faculty of Sciences, Vrije Universiteit Amsterdam, De Boelelaan 1083, 1081 HV Amsterdam, The Netherlands

Received September 19, 2007; E-mail: belp@thch.unipg.it

Abstract: The nature of the chemical bond between gold and the noble gases in the simplest prototype of Au(I) complexes (NgAuF and $NgAu^+$, where Ng = Ar, Kr, Xe), has been theoretically investigated by state of art all-electron fully relativistic DC-CCSD(T) and DFT calculations with extended basis sets. The main properties of the molecules, including dipole moments and polarizabilities, have been computed and a detailed study of the electron density changes upon formation of the Ng−Au bond has been made. The Ar−Au dissociation energy is found to be nearly the same in both Argon compounds. It almost doubles along the NgAuF series and nearly triples in the corresponding $NgAu^+$ series. The formation of the Ng−Au(I) bonds is accompanied by a large and very complex charge redistribution pattern which not only affects the outer valence region but reaches deep into the core−electron region. The charge transfer from the noble gas to Au taking place in the $NgAu^+$ systems is largely reduced in the fluorides but the Ng−Au chemical bond in the latter systems is found to be tighter near the equilibrium distance. The density difference analysis shows, for all three noble gases, a qualitatively identical nature of the Ng−Au bond, characterized by the pronounced charge accumulation in the middle of the Ng−Au internuclear region which is typical of a covalent bond. This bonding density accumulation is more pronounced in the fluorides, where the Au−F bond is found to become more ionic, while the overall density deformation is more evident and less localized in the $NgAu^+$ systems. Accurate density difference maps and charge-transfer curves help explain very subtle features of the chemistry of Au(I), including its peculiar preference for tight linear bicordination.

1. Introduction

In recent years great effort has been expended to prepare and characterize systems in which a noble metal like Cu, Ag, or Au is bound to a noble gas.[1−13] Part of the interest in these systems lies in the old assumption that the elements involved are inert toward forming chemical bonds. Contrary to this suggestion, the chemistry of noble metals is nowadays recognized to be broad and rich. Copper, silver, and gold show an unusual and different reactivity despite belonging to the same group.[14−16] In particular, it is hard to overestimate the modern importance and the singularity of gold chemistry. Gold has the same atomic radius as silver, but its electronegativity and electron affinity are twice as large. These features are manifestations of relativistic effects that contracts and stabilize the *s* and *p* shells, while expanding and destabilizing the *d* and *f* shells.[15] In particular, the noncovalent interaction in dicationic gold dimers is enhanced by the so-called "aurophilicity'', which is a phenomenon that occurs when the soft and expanded 5*d* orbitals interact with each other.[17−20] Gold is in fact generally regarded as the element whose chemistry is most affected by relativistic effects.[15,21] This metal is nowadays used in several high-technology fields, like microelectronics and nanostructured materials science.[22] It is also very important in catalysis[23−25]

§ Universita' di Perugia.
‡ University of Geneva.
|| Vrije Universiteit Amsterdam.

(1) Cooke, S. A.; Gerry, M. C. L. *J. Am. Chem. Soc.* **2004**, *126*, 17000.
(2) Evans, C. J.; Gerry, M. C. L. *J. Chem. Phys.* **2000**, *112*, 1321.
(3) Evans, C. J.; Gerry, M. C. L. *J. Chem. Phys.* **2000**, *112*, 9363.
(4) Evans, C. J.; Lesarri, A.; Gerry, M. C. L. *J. Am. Chem. Soc.* **2000**, *122*, 6100.
(5) Evans, C. J.; Rubinoff, D. J.; Gerry, M. C. L. *Phys. Chem. Chem. Phys.* **2000**, *2*, 3943.
(6) Reynard, L. M.; Evans, C. J.; Gerry, M. C. L. *J. Mol. Spectrosc.* **2001**, *206*, 33.
(7) Walker, N. R.; Reynard, L. M.; Gerry, M. C. L. *J. Mol. Struct.* **2002**, *612*, 109.
(8) Thomas, J. M.; Walker, N. R.; Cooke, S. A.; Gerry, M. C. L. *J. Am. Chem. Soc.* **2004**, *126*, 1235.
(9) Cooke, S. A.; Gerry, M. C. L. *Phys. Chem. Chem. Phys.* **2004**, *6*, 3248.
(10) Michaud, J. M.; Cooke, S. A.; Gerry, M. C. L. *Inorg. Chem.* **2004**, *43*, 3871.
(11) Michaud, J. M.; Gerry, M. C. L. *J. Am. Chem. Soc.* **2006**, *128*, 7613.
(12) Seidel, S.; Seppelt, K. *Science* **2000**, *290*, 117.
(13) Schröder, D.; Schwarz, H.; Hrusak, J.; Pyykkö, P. *Inorg. Chem.* **1998**, *37*, 624.
(14) Descalaux, J. P.; Pyykkö, P. *Chem. Phys. Lett.* **1976**, *39*, 300.
(15) Pyykkö, P. *Chem. Rev.* **1988**, *88*, 563.
(16) Carvajal, M. A.; Novoa, J. J.; Alvarez, S. *J. Am. Chem. Soc.* **2004**, *126*, 1465.
(17) Scherbaum, F.; Grohmann, A.; Huber, B.; Krueger, C.; Schmidbaur, H. *Angew. Chem.* **1988**, *100*, 1602.
(18) Schmidbaur, H. *Gold Bull.* **2000**, *33*, 3.
(19) Pyykkö, P.; Zhao, Y. *Angew. Chem.* **1991**, *103*, 622.
(20) Runeberg, N.; Schütz, M.; Werner, H. J. *J. Chem. Phys.* **1999**, *110*, 7210.
(21) Schwarz, H. *Angew. Chem., Int. Ed.* **2003**, *42*, 4442.

10.1021/ja0772647 CCC: $40.75

and, in this connection, relevant developments concern the catalytic exploitation of Au(I) compounds, which display unique properties governed by relativistic effects.[26] Much studied, as the simplest prototypes for the unconventional reactivity of gold, and in particular of Au(I), are the gold monohalides (see, e.g., ref 27 and ref 28). A special challenge was represented by the AuF molecule, whose existence was questioned for a long time before being eventually characterized in the late nineties.[29−36] The chemistry of gold is thus intensely studied also by theoretical and computational methods (for excellent reviews see refs 28 and 37) and the importance of a deep integration between theoretical and experimental studies has been widely recognized.[21,26]

In 2000, and in fact while searching for AuF, Seidel and Seppelt have synthesized the first bulk compound in which gold is bound to a noble gas (Ng).[12,38−41] This achievement is truly remarkable because it proves the existence of a stable compound between *both* type of elements considered in the past to be archetypes of chemical inertia.[42] In fact, since Bartlett synthesized $XePtF_6$ in 1962,[43] numerous complexes have been made, mostly gas-phase ions, containing a heavy noble gas bound to other elements either covalently or through van der Waals forces. Usually, the more reactive noble gases are Kr, Xe, or Rn, due to their large polarizability and low ionization potential, while the more compact neon and argon atoms are hardly known to form chemical bonds. In fact, great stir was caused, also in 2000, by the discovery of a covalent Ar molecule, HArF.[44]

But what is the nature of the bond between gold and the noble gases? In 1995, Pyykkö predicted the existence of the $NgAu^+$ species by performing pioneering highly correlated CCSD(T) calculations.[45] Based on Mulliken and natural bond analysis at the Hartree−Fock level, he suggested that most of the bonding interaction is covalent in character and strengthens along the Ar−Kr−Xe series. Only half of the bond strength was characterized as electrostatic, based on the known charge-dipole induction formula. This interpretation was questioned by Buckingham et al.,[46] who considered higher order multipoles to describe induced polarization effects on the argon atom. They concluded by saying that "covalency within the $NgAu^+$ species appears to be unproven". To animate the dispute, a recent review of Bellert and Breckenridge[47] suggested, using an electrostatic model and previously calculated parameters,[13,45] that the $XeAu^+$ system is described by a covalent bond in which the noble gas acts as electron donor, while the nature of the bond in other $NgAu^+$ ions was left undecided.[47]

Gerry et al. proposed that the nature of the NgAu bond could be brought to light by exploring the NgMX complexes, with Ng = Ar, Kr, Xe; M = Cu, Ag, Au; X = F, Cl, Br.[1−11] These systems, detected and analyzed using rotational spectroscopy, are linear and present a short Ng−M bond distance. The authors suggested that the complexes with Au show that the bond is more covalent than electrostatic, evidencing that the Ng−Au bond length is smaller than the sum of the covalent radii of Ng and the Au^+ ion. This view was supported by the measurement of the nuclear quadrupole coupling constants, harmonic frequencies, and bond lengths, accompanied by calculations at the second-order Møller-Plesset (MP2) level of theory.

While the work of Gerry et al. just summarized is cutting-edge from the experimental standpoint, the theoretical investigations carried out so far on this kind of systems—and the understanding of their chemical bond—still leave much room for improvement. The calculations of Gerry et al.[1,5,8] and of other authors[48,49] employed the MP2 model, which is known to overestimate the correlation energy, yielding too short bond lengths and too strong closed-shell interactions for these type of systems.[50] Furthermore, the use of effective-core potentials on the heavy nuclei may adversely affect the analysis of the electron density, due to the lack of an explicit core−electron density.[51] Given this state of things, and the interest and importance attached to the chemistry of Au(I) and of the noble gases, in this work we set out to explore, with as much accuracy and detail as is currently feasible, the chemical bond in some of the simplest Au−Ng systems, namely $NgAu^+$ and NgAuF, with Ng = Ar, Kr, Xe. An accurate description of such weak interactions requires the use of methods that describe electron correlation and relativistic effects from the outset, thus necessarily abandoning the familiar orbital picture. We believe that two possible paths can and should be followed, and we explored and compared both in the present work. The first involves the use the most powerful tool known in theoretical chemistry to describe relativity and electron correlation simultaneously, the relativistic coupled cluster model with single and double excitations, including a perturbative correction for the triples, DC-CCSD(T).[52] The second is to make use of Dirac−Kohn−Sham theory[53−55] to describe the electron density and analyze it in detail with appropriate methodologies. This two-pronged approach is of additional particular interest as it also provides a genuine assessment of the validity of DFT on this type of weakly bound systems, which is still largely lacking so far.

The present paper unfolds as follows. We first illustrate, in the next two sections, the methods we have used and some

(22) Leonard, R. M.; Bhuvanesh, N. S. P.; Schaak, R. E. *J. Am. Chem. Soc.* **2005**, *127*, 7326.
(23) Hashmi, A. S. K.; Hutchings, G. J. *Angew. Chem., Int. Ed.* **2006**, *45*, 7896.
(24) Jimènez-Nunez, E.; Echavarren, A. M. *Chem. Commun.* **2007**, 333.
(25) Hamilton, G. L.; Kang, E. J.; Mba, M.; Toste, F. D. *Science* **2007**, *317*, 496.
(26) Gorin, D. J.; Toste, F. D. *Nature* **2007**, *446*, 395.
(27) Brown, J. R.; Schwerdtfeger, P.; Schröder, D.; Schwarz, H. *J. Am. Soc. Mass. Spectrom.* **2002**, *13*, 485.
(28) Pyykkö, P. *Angew. Chem., Int. Ed.* **2004**, *43*, 4412.
(29) Waddington, T. C. *Trans. Faraday Soc.* **1959**, *55*, 1531.
(30) Dasent, W. E. *Nonexistent Compounds: Compounds of Low stability*; Marcel Dekker: New York, 1965.
(31) *Gmelin Handbook, Au Supplement*; Springer: Berlin, 1992; Vol. B1, p 113.
(32) Saenger, K. L.; Sun, C. P. *Phys. Rev. A* **1992**, *46*, 670.
(33) Schröder, D.; Hruak, J.; Tornieporth-Oelting, I. C.; Klapötke, T. M.; Schwarz, H. *Angew. Chem., Int. Ed.* **1994**, *33*, 212.
(34) Evans, C. J.; Gerry, M. C. L. *J. Am. Chem. Soc.* **2000**, *122*, 1560.
(35) Okabayashi, T.; Nakaoka, Y.; Yamazaki, E.; Tanimoto, M. *Chem. Phys. Lett.* **2002**, *366*, 406.
(36) Iliaš, M.; Furdik, P.; Urban, M. *J. Phys. Chem. A* **1998**, *102*, 5263.
(37) Pyykkö, P. *Inorg. Chim. Acta* **2005**, *358*, 4113.
(38) Drews, T.; Seidel, S.; Seppelt, K. *Angew. Chem., Int. Ed.* **2002**, *41*, 454.
(39) Hwang, I. C.; Seidel, S.; Seppelt, K. *Angew. Chem., Int. Ed.* **2003**, *4392*, 42.
(40) Seppelt, K. *Anorg. Allg. Chem.* **2003**, *629*, 2427.
(41) Wesendrup, R.; Schwerdtfeger, P. *Angew. Chem., Int. Ed.* **2000**, *39*, 39.
(42) Pyykkö, P. *Science* **2000**, *290*, 64.
(43) Bartlett, N. *Proc. Chem. Soc.* **1962**, *18*, 1962.
(44) Khriachtchev, L.; Pettersson, M.; Runeberg, N.; Lundell, J.; Räsänen, M. *Nature* **2000**, *406*, 874.
(45) Pyykkö, P. *J. Am. Chem. Soc.* **1995**, *117*, 2069.
(46) Read, J. P.; Buckingham, A. D. *J. Am. Chem. Soc.* **1997**, *119*, 9010.
(47) Bellert, D.; Breckenridge, W. H. *Chem. Rev.* **2002**, *102*, 1595.
(48) Lovallo, C. C.; Klobukowski, M. *Chem. Phys. Lett.* **2003**, *368*, 589.
(49) Lantto, P.; Vaara, J. *J. Chem. Phys.* **2006**, *125*, 174315.
(50) Runeberg, N.; Pyykkö, P. *Int. J. Quantum Chem.* **1998**, *66*, 131.
(51) Bader, R. F. W.; Gillespie, R. J.; Martin, F. *Chem. Phys. Lett.* **1998**, *290*, 488.
(52) Visscher, L.; Dyall, K. G.; Lee, T. J. *Int. J. Quantum Chem* **1995**, *29*, 411.
(53) Rajagopal, A. K.; Callaway, J. *Phys. Rev. B* **1973**, *7*, 1912.
(54) Das, M. P.; Ramana, M. V.; Rajagopal, A. K. *Phys. Rev. A* **1980**, *22*, 9.
(55) MacDonald, A. H.; Vosko, S. H. *J. Phys. C* **1979**, *12*, 2977.

preliminary calculations we have performed to assess as accurately as possible the expected convergence of our results with respect to method and basis set. In section 4 we present and discuss the results we have obtained on the spectroscopic observables, namely bond lengths, dissociation energies, and harmonic frequencies. In section 5 we turn to a discussion of the electronic structure and chemical bond in $NgAu^+$ and NgAuF, first as they may be characterized from properties such as dipole moment, dipole polarizabilities, and atomic charges, and, subsequently, as we have learned from a detailed analysis of the computed one-electron density. A summary and a brief outlook conclude the paper.

2. Methodology

All calculations have been carried out in the relativistic four-component framework. The all-electron DC-CCSD(T) and DC-MP2 calculations were done using the full 4-component Dirac−Coulomb (DC) Hamiltonian, as implemented in the DIRAC program.[56,57] For computational efficiency only the (*LL*|*LL*) and (*SS*|*LL*) two-electron integrals were included. The computed correlation energy in both DC-MP2 and DC-CCSD(T) depends of course on the size of the correlated orbital space. We have chosen to correlate all the electrons corresponding to the full valence of fluorine (7 electrons), the 5p, 5d, and 6s shells of gold (17 electrons), the outermost s and p shells of argon and krypton (8 electrons) and, finally, the 4d, 5s, and 5p shells of xenon (18 electrons). This makes a total of, at most, 42 correlated electrons in the case of the XeAuF system. The active virtual orbital space for correlation was also truncated above an orbital energy of 10 hartree.

All-electron uncontracted basis sets were employed on all atoms. The aug-cc-pVTZ basis set by Dunning [58−60] was used on fluorine and on argon. The triple-ζ quality basis sets (23s16p10d1f) and (28s21p15d1f) by Dyall[61,62] were employed on kripton and xenon, respectively, both of them augmented by a set of 1s, 1p, 1d and 1f functions (exponents for Kr are 0.052, 0.118, 0.126, 0.328 and for Xe are 0.047, 0.042, 0.092, 0.229). On the gold atom, the triple-ζ quality (29s24p15d10f1g) basis set, also by Dyall,[62] was used. We shall refer to the above basis set selection for Ng, Au, and F as VTZ. We carried out a basis set convergence study on the AuF and $ArAu^+$ molecules. To this purpose, in addition to the VTZ described above, we used two other basis sets. The first is a double-ζ quality basis, referred to as VDZ, consisting of aug-cc-pVDZ on F and on Ar[60] and 22s19p12d8f on Au.[61,62] The second is a quadruple-ζ level basis set (VQZ) consisting of aug-cc-pVQZ on F and on Ar[60] and (34s30p19d13f4g2h) on Au.[62]

The density functional theory has been applied in the framework of the Dirac−Kohn−Sham scheme[53−55] as implemented in the program BERTHA.[63−66] The Becke 1998[67] exchange fucntional combined with the Lee−Yang−Parr correlation functional (BLYP)[68] has been used. The topological analysis of the relativistic electron density has been carried out with the program *Mathematica*,[69] which has also been used to produce the density plots discussed in section 5. We also used the ADF package[70−72] to make benchmark studies on the accuracy of the computed vibrational frequencies, by performing scalar zeroth-order regular approximation (ZORA)[73−76] calculations using an all-electron triple-ζ basis augmented by two polarization functions on all the atoms (TZ2P).[72]

Geometrical parameters have been evaluated performing a scan along the Ng−Au and Au−F bond distances. Dipole moments and polarizabilities were calculated at the DC-CCSD(T) level using a finite-field approach, with applied external electric fields of 0, 0.001, and 0.002 au along the molecular axis. Results on these properties at the 4-component DFT-BLYP level were also obtained by linear response theory using the DIRAC code.[56,77,78] The basis set superposition error (BSSE) for the NgAu bond was also evaluated for all complexes using the counterpoise correction of Boys and Bernardi.[79]

3. Preliminary Studies: AuF and $ArAu^+$

To establish a precise context for the accuracy of our calculations, we decided to carry out a preliminary detailed study with various methods and basis sets on the smaller systems AuF and $ArAu^+$. AuF is a particularly appropriate molecule for benchmark calculations since it has been already studied with great detail both experimentally [27,33−35] and theoretically.[27,28,36] Previous calculations on NgAuF have mostly been carried out with relatively small basis sets at the MP2 level[1,5,8,48,49] but the theoretical description of systems involving the weak bond between Au and noble gases is likely to be particularly sensitive to basis set quality and to the level at which electron correlation is accounted for.[13,45] Some investigation of the convergence of the theoretical results is still lacking and clearly desirable. Performing such a convergence study on the adduct systems NgAuF at the all-electron four-component DC−CCSD(T) level with basis sets up to VQZ is clearly impractical. $ArAu^+$ may be considered as a prototype for the Ng−Au bond and, having a particularly small dissociation energy, appears to be the most suitable test systems. Our calculations focused in particular on some critical parameters characterizing the potential energy curves and the bond, namely equilibrium distance r_e, harmonic frequency ω_e, dissociation energy D_e, and the dipole moment μ.

We present first the results obtained for AuF with various methods and the VTZ basis set. As we shall see later, this basis set ensures near-convergence of the results. The results are collected in Table 1, along with previous data from the literature. It has been shown by Iliaš et al.[36] that relativistic effects make the AuF bond less ionic and weaker than would otherwise be expected, because they enhance the electronegativity of gold and reduce electron attraction by fluorine. To describe the AuF bond it is then mandatory to compute accurately the electron affinity of gold, which requires both electron correlation and relativity to be accounted for with great precision. While relativity is nowadays incorporated in an exact formal way by solving the 4-component Dirac equation, the way the electron correlation is handled remains the main source of errors. Thus,

(56) Jensen, H. J.; et al. *DIRAC04, a relativistic ab initio electronic structure program*, release 4.1; 2004. http://dirac.chem.sdu.dk.
(57) Visscher, L.; Saue, T. *J. Chem. Phys.* **2000**, *113*, 3996.
(58) Dunning, T. H. *J. Chem. Phys.* **1989**, *90*, 1007.
(59) Wilson, A. K.; Woon, D. E.; Peterson, K. A.; Dunning, T. H. *J. Chem. Phys.* **1999**, *110*, 7667.
(60) Woon, D. E.; Dunning, T. H. *J. Chem. Phys.* **1993**, *98*, 1358.
(61) Dyall, K. G. *Theor. Chem. Acc.* **2002**, *108*, 335.
(62) Dyall, K. G. *Theor. Chem. Acc.* **2004**, *112*, 403.
(63) Quiney, H. M.; Skaane, H.; Grant, I. P. *Adv. Quantum Chem.* **1999**, *32*, 1.
(64) Grant, I. P.; Quiney, H. M. *Int. J. Quantum Chem.* **2000**, *80*, 283.
(65) Belpassi, L.; Tarantelli, F.; Sgamellotti, A.; Quiney, H. M. *J. Chem. Phys.* **2006**, *124*, 124104.
(66) Quiney, H. M.; Belanzoni, P. *J. Chem. Phys.* **2002**, *117*, 5550.
(67) Becke, A. *Phys. Rev. A* **1988**, *38*, 3098.
(68) Lee, C.; Yang, W.; Parr, R. G. *Phys. Rev. B* **1988**, *37*, 785.
(69) Wolfram, S. *The Mathematica Book*, 4th ed.; Wolfram Media/Cambridge University Press: New York, 1999.
(70) Guerra, C. F.; Snijders, J.; te Velde, G.; Baerends, E. J. *Theor. Chem. Acc.* **1998**, *99*, 391.
(71) te Velde, G.; Bickelhaupt, F.; Baerends, E.; Fonseca Guerra, C.; van Gisbergen, S.; Snijders, J.; Ziegler, T. *J. Comp. Chem.* **2001**, *22*, 931.
(72) *ADF2005.01;* SCM, Theoretical Chemistry Amsterdam, Vrije Universiteit: The Netherlands, http://www.scm.com.
(73) van Lenthe, E.; Baerends, E.; Snijders, J. *J. Chem. Phys.* **1993**, *99*, 4597.
(74) van Lenthe, E.; Baerends, E.; Snijders, J. *J.Chem. Phys.* **1994**, *101*, 9783.
(75) van Lenthe, E.; Ehlers, A.; Baerends, E. *J. Chem. Phys.* **1999**, *110*, 8943.
(76) van Lenthe, E.; Snijders, J.; Baerends, E. *J. Chem. Phys.* **1996**, *105*, 6505.
(77) Saue, T.; Jensen, H. J. A. *J. Chem. Phys.* **2003**, *118*, 522.
(78) Saue, T.; Helgaker, T. *J. Comput. Chem.* **2002**, *23*, 814.
(79) Boys, S. F.; Bernardi, F. *Mol. Phys.* **1979**, *37*, 1529.

Table 1. Computed and Experimental Spectroscopic Constants of the Molecule AuF

	DC-HF	DC-MP2	DC-CCSD(T)	DC-BLYP	exptl [f]
r_e (Å)	1.964[a]	1.886[a] 1.924[b]	1.913[a] 1.918[c]	1.947[a]	1.9184
		1.923[d]	1.947[d]		
ω_e (cm^{-1})	525[a]	597[a] 583[d]	575[a] 555[d] 560[c]	510[a]	563.7
D_e (kJ/mol)	177[a]	302[a]	296[a] 293.7[c] 282.7[d]	324[a]	290
μ (D)	5.77[a]	4.38[a] 4.39[d]	4.29[a] 4.40[d] 4.20[e]	3.69[a]	

[a] This work. [b] Reference 48. [c] Reference 80. [d] Reference 36. [e] Reference 88. [f] Reference 35.

Table 2. Computed Properties of $ArAu^+$ at the DC-CCSD(T) Level with Different Basis Sets (for Details See Section 2)

	ArAu+			AuF		
method	r_e (Å)	ω_e (cm^{-1})	D_e (kJ/mol)	r_e (Å)	ω_e (cm^{-1})	D_e (kJ/mol)
VDZ	2.620	143	36.1	1.933	555	264
VTZ	2.507	167	46.2	1.913	575	296
VQZ	2.477	176	52.8	1.915	569	304

at the DC−HF level of theory, the ionization potential of gold is largely underestimated, by about 150 kJ/mol. Therefore, the AuF bond possesses an unrealistically pronounced ionic character, too large dipole moment and bond length, and too small dissociation energy.

By including electron correlation at the DC-MP2 level, the results improve somewhat over DC−HF (see Table 1), but only at the DC-CCSD(T) level do they get satisfactorily close to the experimental values. The DC-MP2 calculations appear to picture an excessively strong AuF bond, with a too short distance and too large frequency and dissociation energy. Some previous results by other authors using pseudopotentials and smaller basis sets do not show such a clear trend, with the MP2 data, probably because of accidental error cancellations, occasionally in better agreement with experiment than CCSD(T). The calculations by Puzzarini et al.[80] also confirm that electron correlation at the CCSD(T) level and large basis sets are required to achieve quantitative accuracy.

Considering briefly the DFT results, we see in the table that the DC−DFT/BLYP method gives an AuF bond distance too long by about 0.03 Å, an error very similar, but with opposite sign, to the one of the DC-MP2 result. The harmonic frequency is underestimated by about 55 cm^{-1}, while the computed dipole moments is 0.6 D lower than our DC-CCSD(T) figure. This indicates that DC-DFT predicts a slightly less ionic bond compared to explicitly correlated wave function methods.

The other methodological aspect that requires a more systematic assessment than was so far available is the effect of basis set extension. In Table 2 we report the computed spectroscopic observables for AuF and $ArAu^+$ obtained using the DC-CCSD(T) method and the three basis sets detailed in the previous section. For AuF, the table shows clearly that the VDZ basis set produces results still somewhat unsatisfactory.

(80) Puzzarini, C.; Peterson, K. A. *Chem. Phys.* **2005**, *311*, 177.

Table 3. Bond Lengths (Å) of the NgAuF and $NgAu^+$ Complexes

	DC-BLYP		DC–HF	DC-MP2		DC–CCSD(T)		exp[f]	
molecule	r_{NgAu}	r_{AuF}	r_{NgAu}	r_{NgAu}	r_{AuF}	r_{NgAu}	r_{AuF}	r_{NgAu}	r_{AuF}
ArAuF	2.500	1.944	2.659	2.345 2.396[a]	1.886 1.909[a]	2.412	1.908	2.391	1.918
				2.347[b]	1.905[b]				
				2.395[c]	1.949[c]				
KrAuF	2.567	1.950	2.672	2.423 2.454[a]	1.891 1.913[a]	2.487	1.913	2.461	1.918
				2.439[b]	1.910[b]				
				2.452[c]	1.952[c]				
XeAuF	2.657	1.959		2.512 2.545[a]	1.901 1.922[a]	2.573	1.921	2.543	1.918
				2.542[b]	1.918[b]				
				2.562[c]	1.910[c]				
$ArAu^+$	2.523		2.782	2.458		2.507 2.730[d]			
$KrAu^+$	2.565		2.824	2.488		2.537 2.710[d]			
$XeAu^+$	2.654		2.832	2.549		2.609 2.760[d] 2.57[e]			

[a] Reference 48. [b] Reference 49. [c] Reference 1. [d] Reference 45. [e] Reference 13. [f] Ar−AuF from ref 5. Kr−AuF from ref 8. XeAuF from ref 1.

A significant improvement is obtained using the VTZ basis set, while adoption of the VQZ basis offers only tiny additional refinements. As could be expected, the basis set impact on the results for the $ArAu^+$ system, containing a highly polarizable noble gas atom, are more pronounced, but a clear convergence trend is still observed, with the VTZ and VQZ basis set delivering quantitatively similar results. We may reasonably surmise that the quite large VQZ basis produces results close to the basis set limit. A further hint of this comes from considering the BSSE (not accounted for in the table results) which drops from 9 kJ/mol in the VTZ basis to just 2.5 kJ/mol for VQZ. On the basis of these findings, combined with considerations of computational feasibility, it appears that the VTZ basis set represents the best compromise choice between accuracy and cost for our full calculations on the NgAuF systems. Note further that increasing the basis set size appears to strengthen the NgAu bond and, in particular, to reduce the bond length and enlarge the dissociation energy, while BSSE acts in the opposite direction by roughly the same amount. The VTZ BSSE elongates the $ArAu^+$ bond by 0.03 Å. We have found almost identical BSSE figures on both energy and distance for all the compounds studied in this work.

4. The Spectroscopic Constants of NgAuF and $NgAu^+$

We now turn to a discussion of our main results on the series of molecules NgAuF and $NgAu^+$, beginning with the spectroscopic constants: bond lengths, dissociation energies, and harmonic vibrational frequencies. The optimized bond lengths for the NgAuF and $NgAu^+$ series of molecules using different methods are reported in Table 3. The DC-CCSD(T) calculations deliver very accurate values and trends for the parameters of the NgAuF systems. The AuF equilibrium distance is confirmed to be marginally affected by the presence of the weak Au−Ng interaction, remaining in all cases very close (to within less than 0.01 Å) to that of the isolated AuF molecule. The difference is negligible in KrAuF, while there appears to be a very slight contraction of the AuF bond in ArAuF and a similarly small elongation in XeAuF. The DC-CCSD(T) NgAu bond distances are in excellent agreement (to within 0.03 Å) with the values deduced from experiments by assuming the AuF distance fixed

at the free AuF value. The slight difference between DC-CCSD(T) and experiment is in fact nearly constant along the noble-gas series, so that both exhibit essentially identical increments of r_{NgAu}. Note that the increment is nearly the same (0.07−0.08 Å) when replacing Ar with Kr and then Kr with Xe.

Not unexpectedly, the DC-MP2 calculations predict too short bond distances of the NgAuF adducts—by about 0.02 Å for r_{AuF} and 0.06−0.07 Å for r_{NgAu}—compared to DC-CCSD(T). Again we note here that some previous MP2 results (also reported in Table 3), obtained employing pseudopotentials and smaller basis sets, appear, in the light of our calculations, to have been fortuitously accurate. The DFT DC-BLYP model errs in the opposite direction to DC-MP2, predicting too long bond distances by about 0.04 and 0.08−0.09 Å for r_{AuF} and r_{NgAu}, respectively. Remarkably, in both the DC-MP2 and DC-DFT cases these deviations are essentially constant along the series, so that both methods give quite accurate figures for the bond length changes. For completeness, we mention that at the DC-HF level the AuNg bond distances (optimized by keeping the AuF distance fixed at the respective CCSD(T) value) are grossly overestimated, for example, by about 0.25 Å in ArAuF and about 0.19 Å in KrAuF.

It is interesting to compare the AuNg bond distances in the NgAuF adducts with those of the $NgAu^+$ ions, also reported in Table 3. The DC−CCSD(T) calculations show that the bonds are looser in the ions, especially for the lighter ones, as if the addition of a fluorine counterion would actually serve to tighten the bond between gold and the noble gas. We shall return to this interesting point later. The DC-MP2 calculations provide a quite similar picture, only again with significantly underestimated bond lengths (by 0.05−0.06 Å). In stark contrast, the DC-BLYP bond lengths for the ion series are in much better agreement with DC-CCSD(T) than was the case for the NgAuF systems, in fact they are now significantly more accurate than the DC-MP2 results. As a result, there is no appreciable bond tightening on going from $NgAu^+$ to the corresponding fluoride. Some plausible reasons for this DFT behavior will become clearer in the later discussion of the electronic structure. As we found in the fluorides, also in the ions the bond length increases along the series Ar, Kr, Xe, but by quite different amounts: only 0.03 Å upon going from $ArAu^+$ to $KrAu^+$ but more than twice this value, 0.07 Å, from $KrAu^+$ to $XeAu^+$ (CCSD(T) results). In this case, the DC-MP2 and DC-DFT/BLYP calculations give essentially similar trends.

For the $NgAu^+$ ions, an enlightening comparison can be made between the present and previous CCSD(T) calculations performed with quasi-relativistic pseudopotentials and smaller basis sets[45] (results also reported in Table 3). It is seen that the older work predicted bond distances longer than the present results by as much as 0.2 Å, demonstrating the need for large basis sets to describe these weak Au−Ng interactions. This need was already recognized by Schröder et al.[13] and Pyykkö[42] when, by extending the basis set previously used, they obtained for $XeAu^+$ a much smaller bond distance of 2.57 Å,[13] in fact even smaller than our present value of 2.61 Å.

We turn now to a brief illustration of the computed bond dissociation energies, displayed in Table 4. As already observed in previous work,[45,48] all results agree in predicting a large increase in the Ng−Au bond energy in the series Ar, Kr, Xe, both for the NgAuF molecules and for the $NgAu^+$ ions.

Table 4. Computed Dissociation Energies D_e (kJ/mol)

molecule	DC-BLYP	DC-MP2	DC-CCSD(T)
		Ng-Au bond	
ArAuF	31	66	49
		50[a]	
KrAuF	51	87	67
		71[a]	
XeAuF	72	119	94
		97[a]	
$ArAu^+$	60	52	46
			28[b]
$KrAu^+$	98	86	78
			49[b]
$XeAu^+$	153	134	128
		81[b]	88[b]
			126.7[c]
		Au−F bond	
AuF			296
ArAuF			399
KrAuF			406
XeAuF			417

[a] Reference 48. [b] Reference 45. [c] Reference 13.

According to our DC-CCSD(T) calculations, the Ar−Au dissociation energy in both argon compounds is nearly the same (46−49 kJ/mol) and actually slightly smaller for the ion. But while it then almost doubles along the NgAuF series, it nearly triples in the corresponding $NgAu^+$ series, with the results that Kr and, especially, Xe bind substantially more strongly to Au^+ than to AuF. These trends are only in part reproduced by the other theoretical methods, as is best illustrated in Figure 1. We see that at the DC-MP2 level there is a clear inversion in the dissociation energy trends between the fluorides and the ions, with $ArAu^+$ appreciably less bound than ArAuF, $XeAu^+$ more bound than its fluoride by roughly the same amount, and the two krypton compounds almost coinciding. All the DC-MP2 binding energies, in particular those of the fluorides, are substantially larger than the corresponding DC-CCSD(T) values, while the DC−HF values are all grossly underestimated and out of scale. As a result, the trend of dissociation energies for both NgAu+ and NgAuF, upon increasing the level of accuracy of the method employed, follows the "saw-tooth'' pattern already observed by Pyykkö[28] for other closed-shell interactions but not for the $NgAu^+$ systems.[45] In comparing with the available previous theoretical data, we confirm the observations already made when discussing the structural parameters. In particular, previous PP-MP2 results for the fluorides[48] are again found to be, somewhat incongruously, quite accurate, while older PP-CCSD(T) calculations on the ions,[45] largely because of the adoption of a restricted basis set, predicted dissociation energies too small by as much as 30−40%. Basis set extensions led later, for $XeAu^+$,[13,42] to a dissociation energy essentially coinciding with our best result (see Table 4). The DC-DFT/BLYP results show again a peculiarly different pattern in the fluorides and in the ions. Compared to DC-CCSD(T), it underestimates the D_e values of the NgAuF molecules by 17−22 kJ/mol and it overestimates those of the $NgAu^+$ ions by roughly the same amount (14−26 kJ/mol). However, the relative trends of bond strengths within both series of molecules are very well reproduced by the DFT calculations, with dissociation energy differences which deviate from the DC-CCSD(T) ones by about 6 kJ/mol at most.

Experimental determinations of the dissociation energies are not available. However, a way to compare experiment with

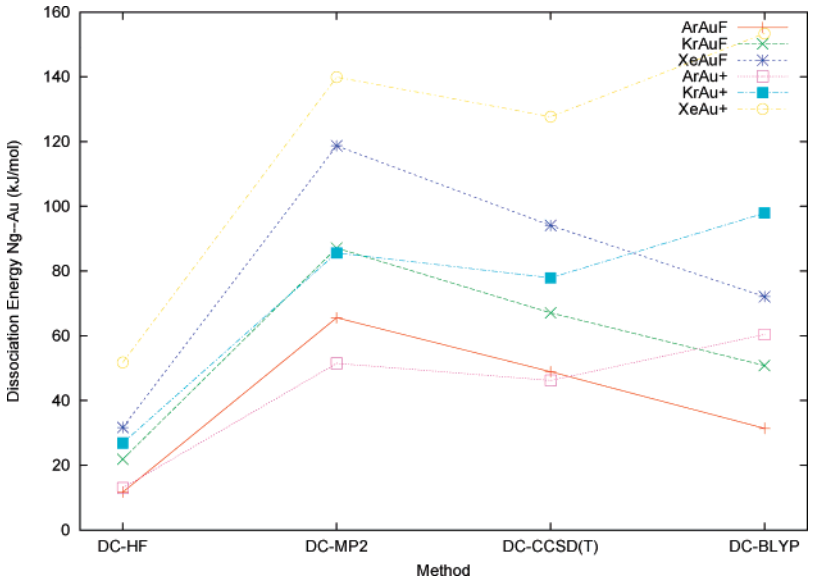

Figure 1. Plot of computed dissociation energies with various theoretical models.

Table 5. Harmonic Frequencies ω_e (cm^{-1}) and Force Constants k ($N \cdot m^{-1}$) of the Ng−Au Bond. The Diatomic Approximation is Used (See Text)

	DC-BLYP		DC–CCSD(T)		exp[c]	
molecule	ω_e	k	ω_e	k	ω_e	k
ArAuF	166	53	203	80	221	97
KrAuF	136	66	163	94	176	110
XeAuF	134	87	156	117	169	137
$ArAu^+$	169	56	167 123[a]	55		
$KrAu^+$	144	72	153 120[a]	81		
$XeAu^+$	142	93	150 129[a] 149[b]	104		

[a] Reference 45. [b] Reference 13. [c] Ar−AuF from ref 5. Kr−AuF from ref 8. Xe−AuF from ref 1.

theory is to compute the force constant of the Ng−Au bond, which has been estimated[1,5,8] from the experimental centrifugal distortion constant and rotational constant in a diatomic approximation, with AuF considered as a single moiety. We preliminarly tested the validity of the diatomic approximation by carrying out a comparison between the analytical evaluation of the Ng−Au vibrational frequencies of the NgAuF complex as a whole and a numerical estimate of the same considering the AuF as a single fragment. We performed these calculations using DFT/ZORA, as implemented in the ADF package.[72] The results confirm very satisfactorily the validity of the diatomic approximation, with frequency values which deviate by at most four wavenumbers. Consequently, we evaluated the Ng−AuF stretching frequencies in diatomic approximation at the DC-CCSD(T) level of theory and, quite satisfactorily, the values obtained are found to agree with the experimentally derived values to within 18 cm^{-1} (see Table 5).

Interestingly, there is a near proportional relation between the force constants of the Ng−Au bond and its dissociation energy, in the NgAuF series as well as in the ionic compounds. However, while, as noted above, the Ng−Au bond energy in the $NgAu^+$ systems is larger than that of the corresponding fluorides (or comparable in the case of the Argon compounds), its force constant (harmonic frequency) is computed to be smaller (or comparable in the case of Xenon). What this finding implies is obviously that, while the charge induced attraction between Au^+ and the noble gas (due to the high polarizability of the latter) is appreciably effective at long-range, making the dissociation energy larger, their interaction is weaker at short distance. In other words, the Ng−Au bond in the vicinity of its equilibrium position is tighter—and shorter (see Table 3)—in the presence of fluorine. The related change in the shape of potential energy curves along the Ng−Au distance is illustrated in Figure 2, where we show a Morse fit of the DC-CCSD(T) data for $KrAu^+$ and KrAuF. The effect of bond tightening induced by fluorine is quite marked in the Argon case and decreases to become almost negligible for Xe. Vice-versa, as we have already seen, the ratio between the bond energy of the ion and that of the corresponding fluoride decreases significantly as the polarizability of the noble gas increases—from 1.06 for Ar to 0.74 for Xe.

A very useful insight into the differences between the NgAu bond in $NgAu^+$ and NgAuF noted above comes from a simple comparative analysis of the electron density in AuF and the Au^+ ion. This is illustrated in Figure 3, where the corresponding density contour plots are displayed. What the figure emphasizes is the surprising fact that, upon formation of the AuF bond, there is, at the gold site, a substantial increase of electron density away from the bond axis and a corresponding decrease along the bond axis, that is, in the direction of approach of the noble gas. Intuitively, this situation favors a closer approach of the electron-donor noble gas and a stronger close-range interaction.

Another interesting and related aspect to consider is the effect of the noble gas on the AuF bond in the NgAuF complexes. We investigated the binding energies between NgAu and the fluorine atom, taking the NgAu fragment at the equilibrium bond distance of the fluoride. We did this by carrying out DC-CCSD(T) calculations on the single-reference doublet $^2S_{1/2}$ ground state of NgAu and on the doublet $^2P_{3/2}$ ground state of the fluorine radical. The results, reported in Table 4, show that the presence of the noble gas increases significantly the energy of the AuF bond. Interestingly, furthermore, the AuF bond energy increases along the noble-gas series, although, as we have seen, to this increment there corresponds a very small geometrical variation

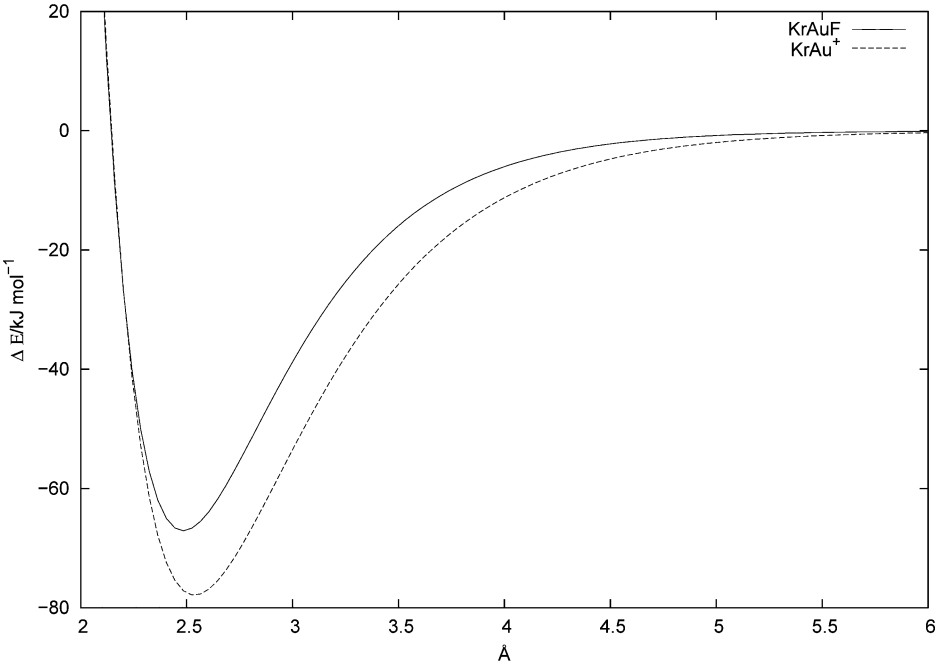

Figure 2. DC-CCSD(T) potential energy curves along the KrAu distance for $KrAu^+$ and KrAuF. For the latter, the AuF bond length is kept fixed at the equilibrium value.

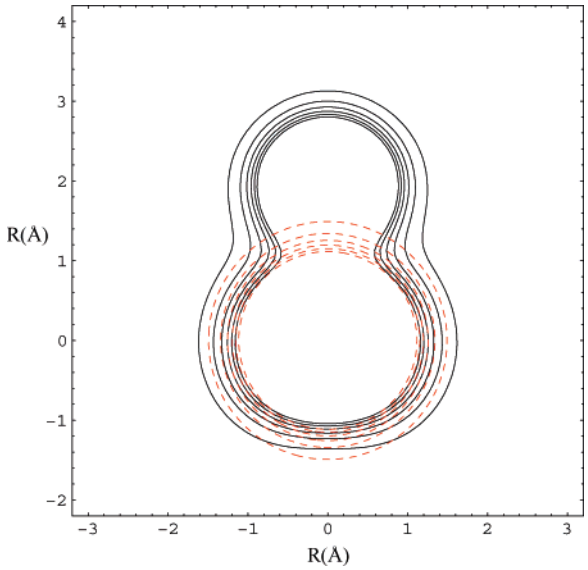

Figure 3. Contour plots of the electron density of AuF (black) and Au^+ (red). The contour levels range from 0.01 to 0.06 e/au^3 with a step of 0.01. Distances are in Å.

(see Table 3 and the accompanying discussion). To cast further light on the nature of the AuF bond in these compounds one may look at the ionization energy (IE) of the neutral NgAu fragments, which we have also computed at the DC-CCSD(T) level. The ArAu moiety has the highest IE (780 kJ/mol), while the KrAu and XeAu fragments can release their electrons more easily, with a IE of 759 and 726 kJ/mol, respectively. The IE of atomic Au is computed to be 875 kJ/mol, in close agreement with the experimental value of 890 kJ/mol.[81] These data suggest that the AuF bond acquires a more ionic character in the presence of a noble gas, which further increases along the Ng series. The study of the electron density presented in the next section will clarify these points.

5. Electronic Structure and Bonding in NgAuF and $NgAu^+$

5.1. Electric Properties: Dipole Moments, Charge Transfer, and Polarizability. In Table 6 we report the computed dipole moments and dipole polarizabilities for the NgAuF and $NgAu^+$ series of molecules. The results for the isolated noble gases, the Au^+ ion and AuF are also shown, together with the available experimental data and previous calculations. Our reference DC-CCSD(T) calculation gives a dipole moment for AuF of 4.29 D, corresponding to an effective positive charge on the gold atom of 0.47. This essentially confirms the result of previous calculations employing the Douglas−Kroll Hamiltonian at the CCSD(T) level.[36] Compared to AuF, the dipole moment increases noticeably in the NgAuF molecules, by 1.46, 1.92, and 2.47 D going down the NgAuF series. Such large changes can hardly be explained by simple electrostatic formulas for charge- or dipole−induced dipole. For the charged $NgAu^+$ species, the absolute value of the dipole moment depends on the origin of the spatial reference system and we show in the table the dipole moments obtained by placing the gold atom at the origin of the coordinates. It is seen that, also for the $NgAu^+$ ions, the dipole moment increases along the Ng series and, not unexpectedly, the increase is more pronounced than in the fluoride series due to more charge-transfer and charge-induced polarization. We may easily define effective charges at the atomic sites that would give rise to the same dipole and such values at the noble gas site are shown in parentheses. We see that the charge effectively doubles along the series from 0.17 in the case of $ArAu^+$ to 0.35 for $XeAu^+$. Thus we find, in accord with Pyykkö,[45] an electron-transfer tendency from the noble gas to the Au^+ ion that increases significantly along the series.

The performance of DFT in the description of the dipole moment and other properties, in particular when transition metals

(81) Lide, D. R. *CRC handbook of Chemistry and Physics*; CRC Press: Boca Raton, FL, 1993.

Table 6. Dipole Moments μ (D) and Dipole Polarizability α (au) along the Internuclear Axis. In Parenthesis Is Reported the Effective Charge Transferred from Ng to Au^+ the Ion

	dipole (D)		polarizability (au)				
system	DC-BLYP	DC-CCSD(T)	DC-BLYP	DC-CCSD(T)	$^c\Delta_{ccsd(t)}$	$^c\Delta_{blyp}$	exptl
Ar			11.5	10.9			11.1[b]
Kr			17.8	16.7			16.7[b]
Xe			29.2	27.3			27.3[b]
Au^+			11.1	11.0			
AuF	3.61	4.29	38.0	36.0			
		4.40[a]		35.9[a]			
ArAuF	5.28	5.75	59.3	51.2	4.3	9.8	
KrAuF	5.81	6.21	70.6	60.9	8.2	14.8	
XeAuF	6.44	6.76	88.6	76.2	12.9	21.4	
$ArAu^+$	2.64 (0.22)	2.08 (0.17)	37.6	31.0	9.1	15.0	
$KrAu^+$	3.73 (0.30)	3.03 (0.25)	49.4	42.1	14.4	20.5	
$XeAu^+$	5.27 (0.41)	4.37 (0.35)	68.4	59.9	21.6	28.1	

[a] Reference 36. [b] Reference 81. [c] Difference between the polarizability of the adducts and the sum of the polarizabilities of the isolated fragments.

and heavy atoms are involved, is well-known to be problematic.[82] In the present calculations we find that DC-BLYP underestimates the dipole moment of AuF and it also slightly underestimates (by 0.47−0.32 D) that of the NgAuF molecules. On the contrary, it overestimates the dipole moment (with respect to the Au center) in the $NgAu^+$ ions. It is thus as if DFT pictures a too electronegative gold, underestimating the ionicity of the AuF molecule and overestimating the charge transfer (by a nearly constant 0.05 electrons) in the $NgAu^+$ systems. Despite these problems, DC-DFT reproduces nearly exactly (to within 0.15 D of the DC-CCSD(T) results) the *changes* in dipole moment, along both the NgAuF and the $NgAu^+$ series. We note that it has recently been similarly found[83] that DFT is capable of predicting reasonably well the changes in the electric field gradient at the gold nucleus for a series of NgAuF systems.

We have also examined the DC-BLYP Mulliken charges of the systems, as well as several other charge analysis results (such as Mulliken, Voronoi, Hirshfeld) as implemented in the program ADF[72] and based on the ZORA Hamiltonian. All these data are available in the Supporting Information. In the case of the $NgAu^+$ series they do not deviate much from the effective charges obtained at the DC-CCSD(T) level, with positive charges on the noble gas in the ranges 0.11−0.17, 0.24−0.27, and 0.31−0.43 for $ArAu^+$, $KrAu^+$, and $XeAu^+$, respectively. The same charge analysis methods applied to the NgAuF molecules result in a much smaller positive charge on Ng, ranging within 0.05−08, 0.10−0.15, and 0.12−0.21 for ArAuF, KrAuF, and XeAuF, respectively. For the latter two systems, previous results by Thomas et al.[8] and Cooke et al.[1] essentially agree with ours. All these results depict an increase of the Ng→Au charge transfer along the noble gas series and are consistent with the corresponding increase in bond strength.

Besides the charge analysis, some information on the electron rearrangement in the complexes NgAuF and $NgAu^+$ with respect to the fragments comes from the computed molecular polarizabilities along the molecular axis, shown in Table 6. Here we note first of all that the theoretical values essentially coincide with the experimental determinations where the latter are available, and in particular for the noble gases. The polarizability is, in both series of Ng−Au molecules, found to increase down the Ng group, reflecting of course the increase in polarizability (a roughly additive property) of the noble gases. More interesting is the analysis of the difference between the polarizability of the adducts and the sum of the polarizabilities of the isolated fragments, also reported in the table. As "fragments'' here we consider again Ng and either the Au^+ ion or AuF. The first eye-catching feature is that, in all cases, the polarizability difference is largely positive. Thus, the electrons in the molecules are much more mobile (along the internuclear axis) than in the isolated fragments, suggesting the more pronounced delocalization associated with the formation of loose covalent bonds. Furthermore, this difference increases, both in absolute and in relative terms, down the noble gas series, more markedly for the $NgAu^+$ ions than for the NgAuF molecules. These results correlate remarkably well with the results of the charge analysis discussed earlier. The polarizability results obtained with the DC-BLYP method, as already noted for the dipole moments, show some significant deviations from DC-CCSD(T) in the absolute values but, again, they reproduce quite satisfactorily the qualitative trends.

5.2. The Ng−Au Bond. A Detailed Study of the Electron Density. Previous works on the NgAuF systems have sketched a picture of the bonding based on an analysis of the individual orbitals.[1,8] Here we would like to focus essentially on the conclusions that may be drawn by studying the total relativistic, correlated, one-electron density. Among other popular methods of analysis that have been reported in the literature aimed at rationalizing chemical bonds, are the topological analysis of the electronic density, mainly developed in the framework of the theory of atoms in molecules (AIM) of Bader et al.,[84] and methods based on fragment energy decompositions.[71] Neither methodology (detailed results have been collected in the Supporting Information) appears capable of providing a sharp and simple characterization of the Ng−Au interaction in the complexes under study. We summarize in the following the main results.

A bond critical point (bcp), that characterizes a chemical bond in the framework of AIM theory,[84] is found for the Ng−Au bond in all complexes. The electronic density at the bcp is found to increase along the Ng series, with values only slightly smaller

(82) Schwerdtfeger, P.; Pernpointner, M.; Laerdahl, J. K. *J. Chem. Phys.* **1999**, *111*, 3357.
(83) Belpassi, L.; Tarantelli, F.; Sgamellotti, A.; Götz, A.; Visscher, L. *Chem. Phys. Lett.* **2007**, *442*, 233.
(84) Bader, R. F. W. *Atoms in Molecules. A Quantum Theory*; Cambridge University Press: Oxford, 1991.

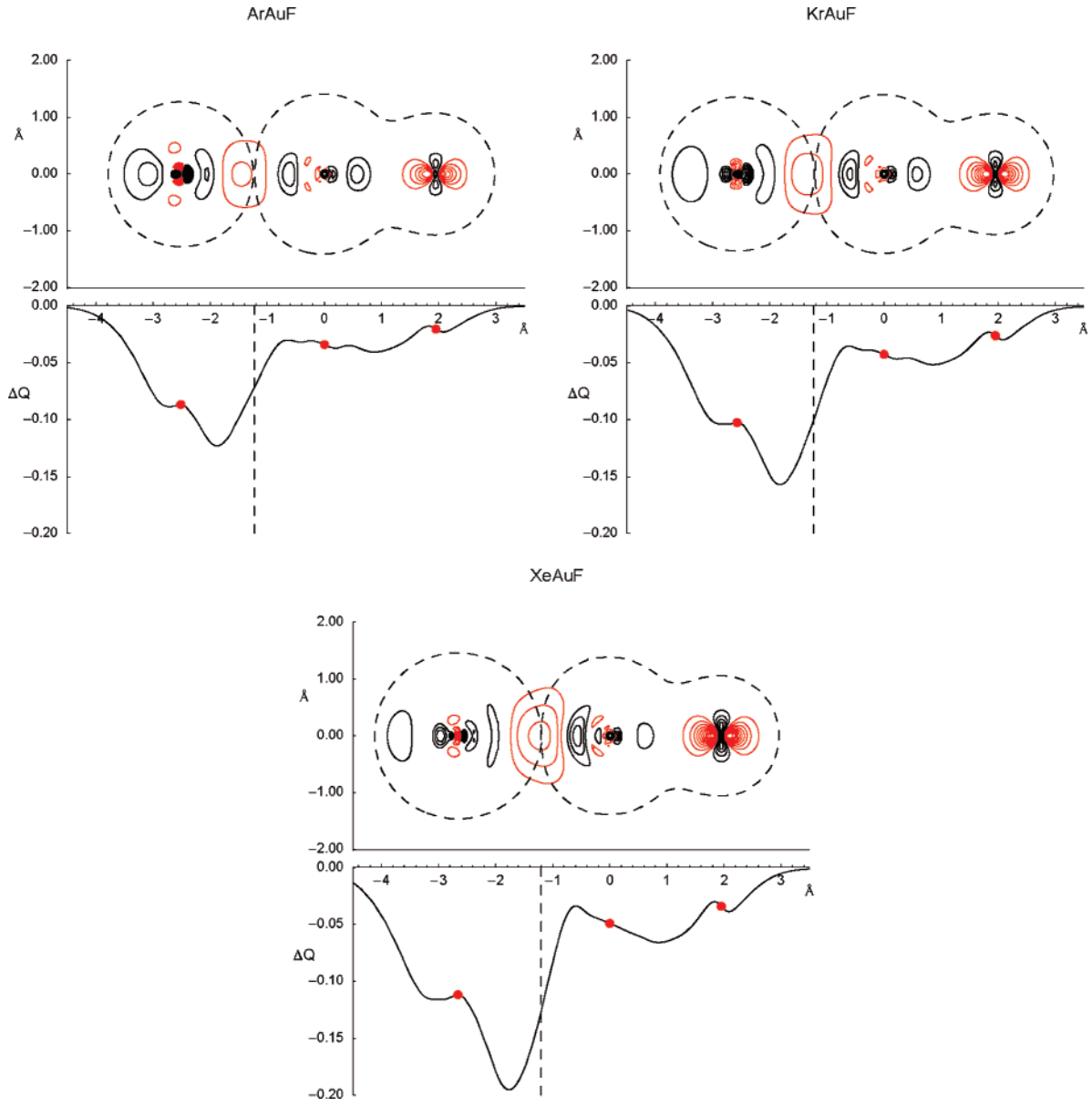

Figure 4. Contour plots of the electron density difference between NgAuF molecules and the Ng and AuF fragments. The positive contour levels (red) range from 0.005 to 0.2 e/au^3 with a step of 0.005, while the negative ones (black) range from −0.005 to −0.2 e/au^3 with a step of 0.005. In the bottom part the integrated charge tranfer ΔQ (see text) is reported as a function of the internuclear distance.

than has been found for the strong Au−Au bond in the Au_2 molecule (0.083 e/(au)^3).[85] As a general feature we observe that not only the electron density but all the topological parameters change smoothly along the Ng series both for the NgAuF and $NgAu^+$ complexes. All bonds (bcps) are characterized by small absolute values of the density Laplacian (positive in all cases), total energy density, kinetic energy density, and potential energy density. Interestingly, the (negative) potential-energy contribution to the total energy density increases monotonically along the noble gas series both for the NgAuF and $NgAu^+$. This is interpreted as implying that the tendency of the electronic density to build up at the bcp increases down the series. A feature that has been associated to the covalent character of a bond is a negative value of the energy density at the bcp. In the case of our series of molecules, slightly negative values of the energy density have been found for both Xenon compounds and for $KrAu^+$. However, as we said above, the values of all the principal topological parameters are very small and change very smothly from molecule to molecule, making any sharp distinction in the nature of the bond for the three noble gases seem quite unrealistic.

As a more qualitative but more insightful approach to understanding the nature of the Ng−Au interaction we decided to look at a graphical representation of the changes in the electron density upon formation of the chemical bond between the fragments. This approach is particularly consistent from a theoretical point of view because both fragments and complexes are closed shell molecules. In Figure 4 and Figure 5 we report the contour plots of the DC-BLYP electron density difference between the complexes and the non-interacting fragments (in the same positions) for the NgAuF and the $NgAu^+$ series, respectively. The red contours refer to positive differences

(85) Belpassi, L.; Tarantelli, F.; Sgamellotti, A.; Quiney, H. M. *J. Phys. Chem. A* **2006**, *110*, 4543.

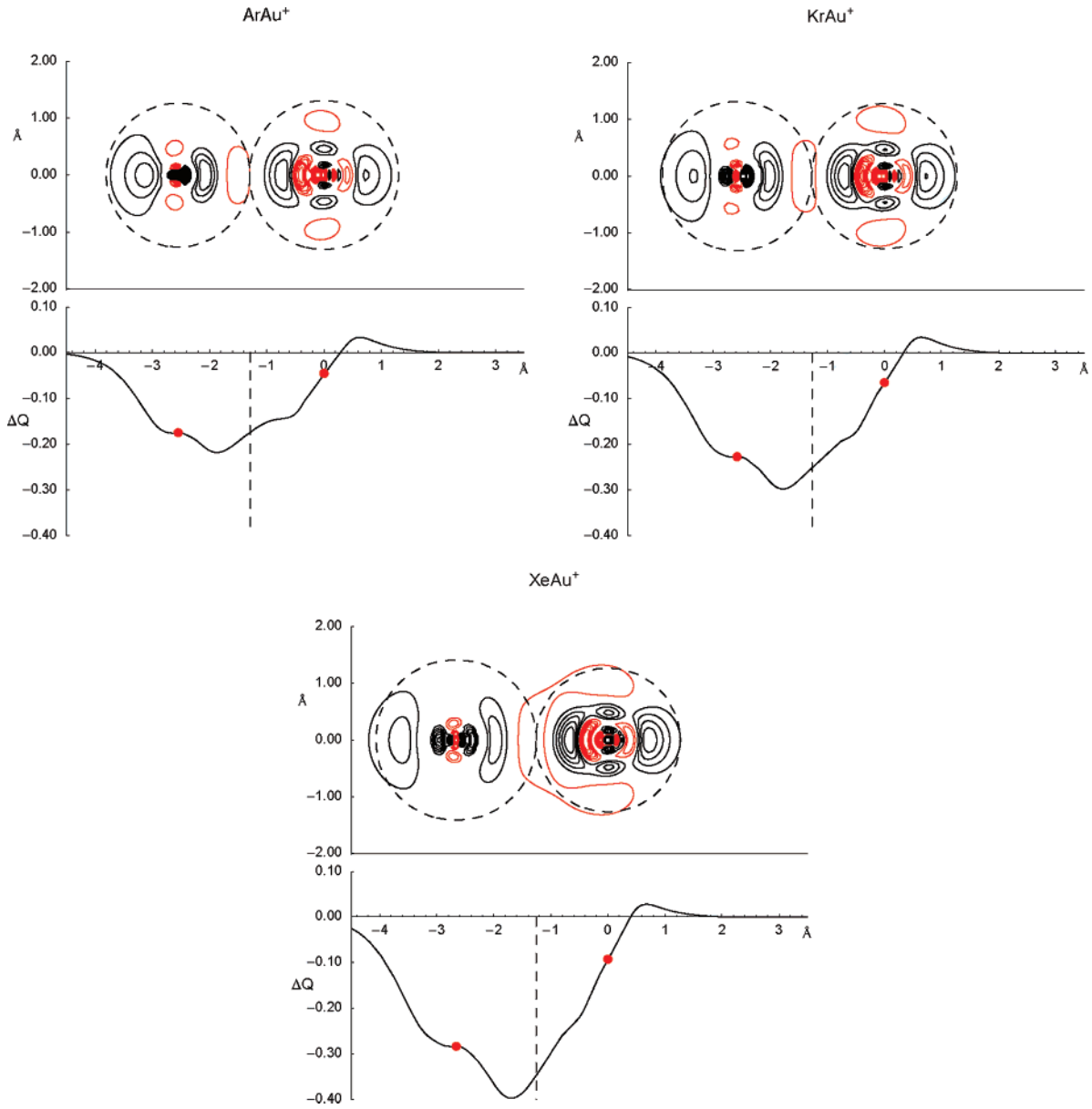

Figure 5. Contour plots of the electron density difference between $NgAu^+$ molecules and the Ng and Au^+ fragments. The positive contour levels (red) range from 0.005 to 0.2 e/au^3 with a step of 0.005, while the negative ones (black) range from −0.005 to −0.2 e/au^3 with a step of 0.005. In the bottom part the integrated charge tranfer ΔQ (see text) is reported as a function of the internuclear distance.

(density accumulation) and the black contours are negative ones (density depletion). The dashed contour marks the isodensity value of both isolated fragments which crosses the internuclear axis at the same point and may thus serve to visualize tangent boundaries enclosing the non-interacting fragments.

The first eye-catching and surprising feature, common to all the plots, is their very rich structure, indicative of a rather complex rearrangement of the electronic density taking place when Au^+ or AuF binds a noble gas atom. The extent of the density deformation appears to increase on going from the lighter to the heavier Ng atom. Another quite remarkable general feature of the density changes, which is brought to light thanks to the all-electron nature of our calculations, is that the valence electron rearrangement upon bond formation has very large repercussions in the core−electron region closer to the nuclei, especially at the gold site. Incidentally, this provides a clear qualitative explanation of the particularly large nuclear quadrupole coupling constants observed for the NgAuF complexes.[1,5,8]

Concerning the Ng−Au interaction, the most significant feature emerging from the density difference plots is the evident accumulation of electronic charge in the region between the Ng and Au nuclei. Note that this density increase appears to be centered surprisingly close to the point of contact of the tangent fragment boundaries chosen above. It is remarkable that this region of density increase is delimited, on both sides along the internuclear axis, by a region of density depletion. In other words, there appears to be a net transfer of electron density toward the outer valence region between the noble gas and the gold nuclei, with formation of a weak covalent chemical bond. This behavior is qualitatively observed for all complexes studied here, increasing in extent as one moves from Ar to Xe.

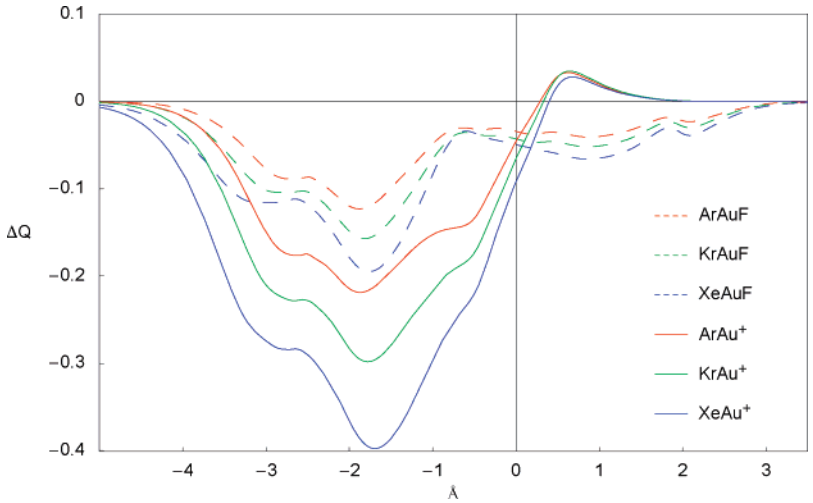

Figure 6. The integrated charge tranfers ΔQ (see text) are reported as a function of the internuclear distance for all NgAuF and $NgAu^+$ complexes.

In comparing the contour plots for the corresponding NgAuF and $NgAu^+$ systems, we note first of all that the density accumulation in the Ng−Au internuclear region is more pronouced in the fluorides but the ions present a generally larger and much less localized density deformation. These pictures appear to match qualitatively well the different trends in the bond force constants and bond dissociation energies discussed earlier. Within the boundary enclosing the noble gas the density change is essentially identical in shape, only appreciably more pronounced in the ion case. On the gold side, by contrast, there is a more evident qualitative difference in the density distortion maps. In particular, we note that in NgAuF the density moves mostly along and in the vicinity of the internuclear axis while in the corresponding $NgAu^+$ ion there are significant charge shifts also in the direction perpendicular to the axis at the gold site.

A quite spectacular and surprising feature emerging from the $NgAu^+$ plots is that, despite the overall charge transfer from Ng to Au^+ which we have discussed earlier (and which is in fact overestimated in the DC-BLYP picture), there is a large drop in electron density on the far side of the gold atom opposite to the noble gas. This may essentially be seen as making gold more of an electron attractor than free Au^+ toward an atom approaching from this side and explains quite nicely, in terms of the sole electron density, the finding of Pyykkö[45] that the $NgAuNg^+$ molecules have a remarkably strong and short NgAu bond. Note that the $NgAuNg^+$ species is isoelectronic with NgAuX, where X is the immediately preceding halide. This peculiar density change at the gold site, if general, could be at the origin of the recognized preference of Au(I), compared to other homologues such as Cu(I) and Ag(I), for linear bicoordination.[16,26,86,87]

Considering finally the density change more closely involving the fluorine atom upon formation of the NgAu bond in NgAuF, the plots visually confirm that the internuclear region of the AuF bond is uniformly and relatively little affected. Somewhat surprisingly, the largest effect of the complex formation is at the fluorine site, which is electron enriched and polarized almost symmetrically along the molecular axis.

To make the picture of the bonding which emerges from the density difference plots more quantitative, we show, below each one, the curve representing the partial integral of the density difference along the internuclear axis. This thus measures the actual electronic charge fluctuation with respect to the isolated fragments, as one moves from left to right along the internuclear axis (z) and is defined as follows:

$$\Delta Q(z) = \int_{-\infty}^{\infty} dx \int_{-\infty}^{\infty} dy \int_{-\infty}^{z} \Delta\varsigma(x,y,z')\, dz' \qquad (1)$$

where $\Delta\varsigma$ is the electron density of the complex minus that of the two isolated fragments. The same plots are also all collected, for better comparison, in Figure 6. The red dots on the curves in Figures 4 and 5 mark the nuclear positions, while the dashed vertical line marks the fragment boundary defined earlier.

Imagining each point on the internuclear axis to identify a perpendicular plane passing through that point, the corresponding value of ΔQ measures the amount of electronic charge that, with respect to the situation in the non-interacting fragments, has moved from the right side to the left side of the plane. Thus a negative value indicates a charge transfer of that magnitude from left to right. The difference between two ΔQ values gives the net electron influx into the region delimited by the corresponding two planes. Thus, the regions of the ΔQ curve where the slope is negative correspond clearly to zones of charge depletion (black contours), while charge accumulates where ΔQ picks up (red contours).

Looking first at the NgAuF graphs in Figure 4, the first thing one notices is that ΔQ is negative everywhere in the molecular region, indicating that, at each point, there has been a net shift of charge toward the fluorine end. This is in fact true even to the right of the fluorine position, in accord with the polarization of fluorine observed earlier. The plots make clear the pronounced electron depletion around the Ng site and the charge transfer to the Ng−Au internuclear region, which increases along the noble gas series. For all noble gases, the pattern of charge transfer is essentially identical: the electron loss takes place until about 1.8 Å from the gold site, where there is a rather sharp inversion and charge starts to re-accumulate rapidly until

(86) Orgel, L. E. *J. Chem. Soc.* **1958**, 4186.
(87) Schwerdtfeger, P.; Hermann, H. L.; Schmidbaur, H. *Inorg. Chem.* **2003**, *42*, 1334.
(88) Pitonák, M.; Neogrády, P.; Kellö, V.; Urban, M. *Mol. Phys.* **2006**, *104*, 2277.

about 0.8 Å, when most of the lost charge (to within less than 0.04 electrons) is recovered. To the extent that the isodensity contour chosen above as delimiting the Ng and AuF fragments has any realistic meaning, we may interpret $|\Delta Q|$ at the point of contact (vertical dashed line) as an estimate of the charge transferred from Ng to AuF. This value is in fact in quite close agreement with the charge analysis results, increasing from about 0.07 for ArAuF to 0.10 for KrAuF and 0.12 for XeAuF. In the region roughly 2 Å wide centered at the gold atom, the curves have negative slope but are relatively flat, corresponding to a small net electron depletion which becomes more prononuced from the Ar to the Xe complex. The charge increases instead around the fluorine atom. This suggests an increased ionic character of the AuF bond in the complexes and thus supports the hypothesis formulated earlier on the basis of the electron affinity of the $NgAu^+$ ions (IE of NgAu).

In the case of the $NgAu^+$ complexes, the plots evidence that the charge transfer from the noble gas is much more pronounced than in the fluorides, but again it follows the same qualitative pattern for all three noble gases. In addition, the charge is transferred not only to the internuclear region but also to the region surrounding the gold atom itself, which may be interpreted as the partial filling of the empty 6s orbital. Interestingly, we note to the right of the gold nucleus a narrow zone where ΔQ becomes positive, implying a corresponding net electron depletion to the right of this zone which, as we have surmised from the contour plots, makes the gold site in $NgAu^+$ more electrophilic than Au^+ itself. We may finally again note the interesting detail that the charge-transfer values at our chosen fragment boundary (vertical dashed line) are qualitatively consistent with the charge analysis results discussed earlier (0.17, 0.25, and 0.35 for $ArAu^+$, $KrAu^+$ and $XeAu^+$, respectively).

The complex structure of the density changes in the $NgAu^+$ complexes and the trends in bonding can to some extent also be rationalized in a simple orbital picture. To this end we carried out a fragment analysis calculation using the ADF package[72] (see the Supporting Information). As fragments we considered the neutral Ng atoms and the remainder in both series of complexes. A simple qualitative picture that explains the density difference visible in Figure 3 is that in AuF the $5d_{z^2}$ and 6s orbitals mix with the fluorine $2p_z$ orbital. This hybridization moves charge into the AuF bonding region, leading to a depletion on the other side of the gold nucleus. The result is a smaller Pauli repulsion energy in NgAuF relative to $NgAu^+$. In simple terms one may say that the hybrization energy necessary to have the Ng approach the gold ion more closely is already paid by the fluorine. In $XeAu^+$ Mulliken analysis furthermore indicates the presence of a 0.15 e "5d hole" on gold that correlates well with the 5d feature visible in Figure 5. This 5d hole is in $NgAu^+$ induced by the formation of the Au-Ng bond, while it is already present in AuF in case of the NgAuF complex.

6. Summary and Conclusions

The desire to understand and rationalize chemical bonds is a fundamental motivation of chemical research and a case in point is the extremely interesting and much studied chemical bond between the archetypal noble metal, gold, and the noble gases (Ng), the elusive nature of which has long defied analysis. In the present work we have taken up the challenge of settling, to the best of current theoretical and computational possibilities, this question, by a detailed all-electron, fully relativistic DC-CCSD(T) and DFT study of the adducts between two of the simplest Au(I) species, namely Au^+ and AuF, and the noble gases Ar, Kr, and Xe. The bond energies and the principal structural, spectroscopic, and electric properties of the six molecules have been calculated by DC-CCSD(T) using a triple-ζ basis set combined with a basis set convergence study, while an in-depth analysis of the electron density changes occurring upon formation of the Ng−Au bonds has been made by 4-component Dirac−Kohn−Sham calculations. The resulting theoretical picture we obtained of the electronic structure of these systems is the most accurate and reliably achievable today, permitting a detailed understanding of the nature of the bond and the clarification of some of its most peculiar apects.

The Ng−Au bond energy in both complexes NgAuF and $NgAu^+$ is found to increase going down the series (Ng = Ar, Kr, Xe). The Ar−Au dissociation energy is nearly the same (46−49 kJ/mol) in both argon compounds. But while it then almost doubles along the NgAuF series, it nearly triples in the corresponding $NgAu^+$ series, with the results that Kr and, especially, Xe bind substantially more energetically to Au^+ than to AuF. While this may clearly be related to the different polarizability of the noble gases, it is somewhat surprisingly found that the bond force constants (harmonic frequencies) follow the opposite trend, being larger in the fluorides than in the corresponding ions. The Ng−Au bond lengths are correspondingly shorter. A comparative analysis of the electron density reveals a simple origin for this unexpected feature. Upon formation of the AuF bond, there is, at the gold site, a substantial increase of electron density away from the bond axis and a corresponding decrease along the bond axis, that is, in the direction of approach of the noble gas. This situation favors a closer approach of the electron-donor noble gas and a stronger close-range interaction.

As previously correctly assumed, the calculations confirm that the AuF bond length is only very slightly affected by the interaction of gold with the noble gases. However, the AuF dissociation energy increases appreciably and the results suggest that the AuF bond becomes more ionic in the presence of the noble gas, a trend which is more evident with the heavier ligands. Various methods of population analysis based on our calculations, as well as the study of the dipole moments and polarizabilities, indicate that the NgAu bond in $NgAu^+$ is characterized by an appreciable charge transfer from the noble gas toward gold. The computed positive charge on Ng is 0.11−0.17 in $ArAu^+$, 0.24−0.27 in $KrAu^+$, and 0.31−0.43 in $XeAu^+$. In the corresponding fluorides the Ng charge is smaller by as much as 50−60%.

The maps of electron density deformation upon formation of the Ng−Au bond, and the corresponding charge-transfer curves along the internuclear axis, evidence an extremely complex and far-reaching density rearrangement pattern which is largely unexpected for such weak interactions. Besides large changes in the density of the outer valence region, the inner-valence and even the deep core−electron region, both at the noble gas and gold sites, are significantly affected, with alternating zones of density accumulation and depletion. Even the electron density at the fluorine site in NgAuF is strongly distorted.

The main feature of the bond is a pronounced charge accumulation in the middle of the region between the Ng and Au nuclei, delimited on both sides by a zone of charge depletion particularly marked at the noble gas. This feature is a clear indication of the formation of a polar covalent bond and confirms some previous suggestions made for the $NgAu^+$ ions.[45,47] It is a remarkable finding of the present work that such bond-formation pattern is identical in all systems studied, thus including the most inert argon atom, only becoming more pronounced as one moves from Ar to Xe. The density maps show that the density accumulation in the Ng−Au internuclear region is also more marked in the fluorides than in the corresponding $NgAu^+$ ions but, by contrast, the density deformation in the latter is generally more pronounced and less localized to the bond region. The charge-transfer curves confirm in detail the appreciable electron transfer from the noble gas. Notably, in the ionic systems, this charge transfer is not limited to the internuclear region but extends to the region of the gold atom itself. The picture emerging from the density maps thus explains well the different trend of dissociation energies and force constants.

An interesting feature brought to light by the density-difference maps and charge-transfer curves is that, despite the overall significant charge transfer from the noble gas to Au^+ in the formation of $NgAu^+$, there is a large drop in electron density on the far side of the gold atom opposite to the noble gas. This may essentially be seen as making gold more electrophilic than free Au^+ toward an atom approaching from this side. If general, this peculiar density change at the gold site could be at the origin of the recognized preference of Au(I), compared to other homologues such as Cu(I) and Ag(I), for linear bicoordination and the peculiar catalitic properties of Au(I) complexes. This aspect clearly deserves further research along the lines adopted in the present work.

Acknowledgment. L.B. and I.I. thank the Project HPC-EUROPA (RII3-CT-2003-506079), with the support of the European Community-Research Infrastructure Action under the FP6 "Structuring the European research Area" Program. This work has been partially supported by FIRB 2003 "Molecular compounds and hybrid nanostructured materials with resonant and nonresonant optical properties for photonic devices".

Supporting Information Available: Complite author list for ref 56; charge and topological analysis and energy decomposition results. This material is available free of charge via the Internet at http://pubs.acs.org.

JA0772647